

# 3-PHASE FULL BRIDGE CONVERTER BASED SRM FOR CLOSED LOOP CONTROL OF AN ELECTRIC VEHICLE

K. Akhila Reddy<sup>1</sup>, Dr. G.Venu Madhav<sup>2</sup>, Dr. C. Nagamani<sup>3</sup>, Dr. T. Anil Kumar<sup>4</sup>

<sup>1</sup>PG Student, <sup>2</sup>Associated Professor, <sup>3</sup>Associated Professor, <sup>4</sup>Professor

<sup>1, 2, 3, 4</sup>Department of Electrical and Electronics Engineering, Anurag University, Venkatapur, Ghatkesar, Medchal–Malkajgiri district, Hyderabad, Telangana, India. 500088

<sup>1</sup>reddy.akhila99@gmail.com, <sup>2</sup>venumadhav@anurag.edu.in, <sup>3</sup>nagamani@anurag.edu.in, <sup>4</sup>thalluru@anil@gmail.com

**Abstract:** In this paper a SRM is operated using different control circuits which include a) AHBC b) AFBC c) AHBC with closed loop control. In all the control modules the machine used is the same three phase 6/4 SRM machine. A performance analysis is carried out on SRM with these different circuits and the analysis is compared for best performance module selection. The modeling of these proposed modules is designed in MATLAB Simulink software for result validation with generation of graphs using 'powergui' toolbox. The plotted graphs for the comparison are always with respect to time.

**Keywords:** SRM (Switched Reluctance Motor), MATLAB (Matrix Laboratory), powergui (power graphical user interface).

## 1. Introduction

Utilization of better performance motors with high efficiency in electric vehicles is increasing day by day. Different machines like PMSM (Permanent magnet synchronous motor), BLDC (Brushless DC motor), and Induction motors are used for traction purposes. However, these machines might be less efficient and very difficult to be controlled with complex controllers. As compared to these machines SRM [1] (Switched Reluctance Motor) is considered to be simple in structure with simple construction of stator and rotor of the machine. Even the efficiency of SRM is higher as compared to the above-mentioned motors. The range of the speed is also very good which can vary from low speeds to very high speeds. This makes the motor more economical and simpler to control with better cooling system which can be an added advantage for electric vehicle applications [2]. The rugged structure of the motor makes it more reliable which is the major priority for an electric vehicle as it used for transportation purpose. This reduces the cost of the vehicle, increases reliability, improves efficiency, reduced control complexity as compared to traditional motors used in electric vehicles.

As that of the other motors which were mentioned earlier even the SRM needs to be controlled by power electronic circuits

[3] [4]. There are many converter types for controlling the SRM which include a) Asymmetric half bridge converter (AHBC) b) Asymmetric full bridge converter (AFBC) c) AHBC with closed loop control. The AHBC and AFBC are conventional circuits which are operated with no feedback from the motor. The conventional asymmetric half bridge and asymmetric full bridge converters [4] are shown in figures 1 and 2.

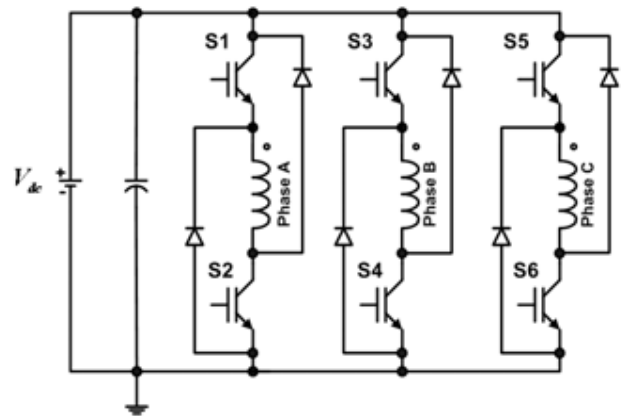


Fig. 1: AHBC for SRM

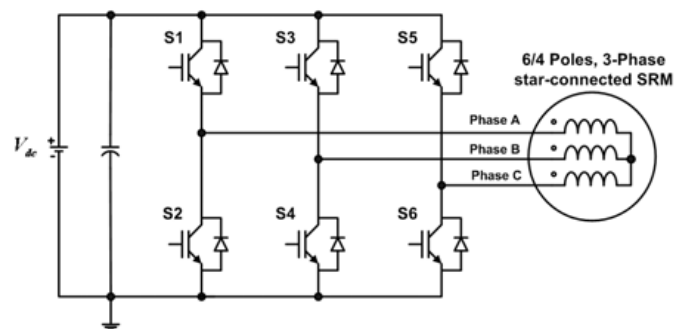


Fig. 2: AFBC for SRM

In both the bridges six power electronic devices (IGBTs) are used with two switches [5] in each leg. In the AHBC the SRM machine winding is placed between switches of the same leg for conduction of current through the phase winding for excitation. The other two phases are similarly placed between other two legs of the converter. But in AFBC the other end of

the SRM windings are neutralized [5] and the inputs of the windings are connected to each leg of the six switch converter. Both the converters are controlled by control signals which are generated in sequence with respect to the stator winding mechanical angle. For the speed control of the SRM motor, a novel feedback closed loop control structure [6] is adopted with speed feedback from the motor. A symmetric full bridge converter is utilized for this purpose which is controlled by the feedback loop control system.

The paper is categorized into section II comprising of SRM operation and converter working principle, followed by section III discussing about controller's design. In section IV the simulation results and discussion of the proposed modules are given with time reference graphs plotted for different operating conditions. In the final section V conclusion for the paper followed by references used to write this paper are mentioned.

**2. Converters Operating Principle**

As previously mentioned the converters used for controlling SRM include IGBT power electronic switches which are controlled by sequential pulses with respect to the stator poles. The motor used of the analysis is 6/4 SRM [7] which represents (6 stator poles and 4 rotor poles). The internal construction of the considered SRM is shown in figure 3.

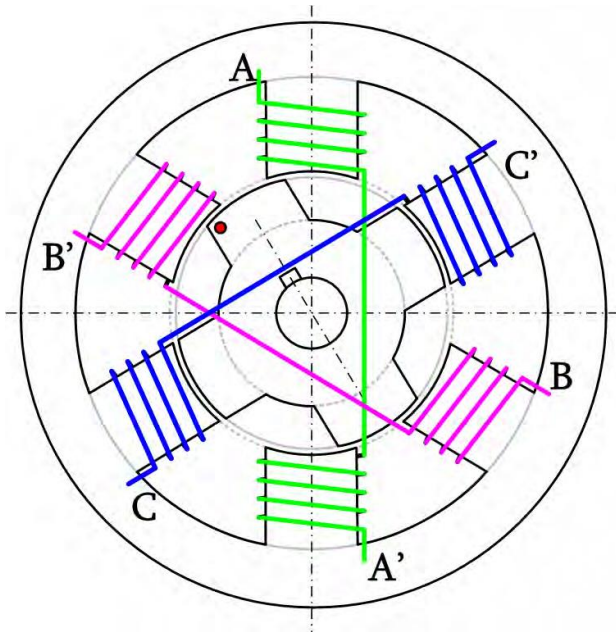


Fig. 3: 6/4 SRM internal structure

For the half bridge asymmetric converter module in figure 1 the A terminal of SRM is connected to emitter terminal of switch S1, and A' terminal of SRM is connected collector terminal of switch S2. In similar way the BB' and CC' windings are connected in the other two legs of the converter. During the conduction of switches S1 and S2 the current passes through AA' making it magnetically excited with magnetic N-pole assigned to A pole and magnetic S-pole A'

pole [7]. The rotor moves away from this position because of the repulsive force because of opposite poles of stator and rotor. In order to continue the movement, the next pulse is fed to BB' and next to CC' continuously.

As for the full bridge asymmetric converter the A'B' and C' terminals of SRM are connected to common point representing as neutral. And A B and C are the input terminals of the machine connected between the switches in each leg as in figure 2. The six switches pulses are synchronized in such a way that one pole is activated each time during the rotation. The commutation signals are produced as per the mechanical angle between the poles. For positive current condition in the machine winding the upper region switches S1 S3 and S5 are switches ON and for negative current conduction in the machine winding the lower region switches S2 S4 and S6 [8] are switched ON. The switching sequence is changed for every 30 degrees of mechanical angle during the rotation of the rotor. In order to avoid short circuit the two switches in the same leg operate with very high phase difference excitation maintaining the machine continuous operation. Due to this gap in the excitation sequence there is conduction gap in the winding which causes ripple in the speed of the machine reducing the reliability and efficiency of the complete module. This issue is overcome in the symmetric full bridge converter which comprises of freewheeling diode switches for no gap in the excitation sequence.

**3. Controllers Design**

The pulse generations for the converters are discussed in this section with open loop and closed loop structures. Initially open loop pulse generation is modeled by using simple pulse generators for the IGBTs connected in the circuits. The switching sequence of one full cycle for the AHBC can be seen below.

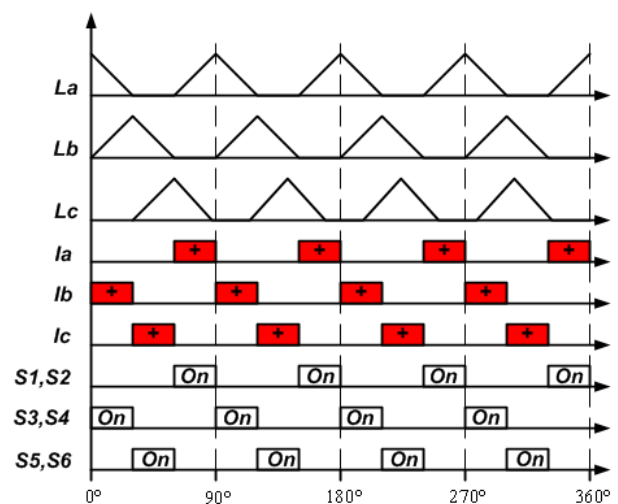


Fig. 4: Switching sequence for AHBC

As seen in the above figure the signals for switches S1S2, S3S4 and S5S6 switches are common [9] which operate

simultaneously. The signal for the switches decides the current passing through the phase windings. When the switches S1 and S2 are switched ON simultaneously current Ia passes through stator inductor La exciting the phase A winding. After 30 degrees conduction of S1 and S2 the signal is turned OFF and the next leg switches S3 and S4 of phase B are turned ON. This excites the phase B stator winding for another 30 degrees with inductor current Ib. The pulse further continues for next stator winding phase C with switching ON the switches S5 and S6. The sequence repeats for every 90 degrees and repeats for 4 times in 360 degrees cycle. The gap between the pulses is determined by the number of stator poles. The pulse sequence generation for AFBC can be seen below in figure 5.

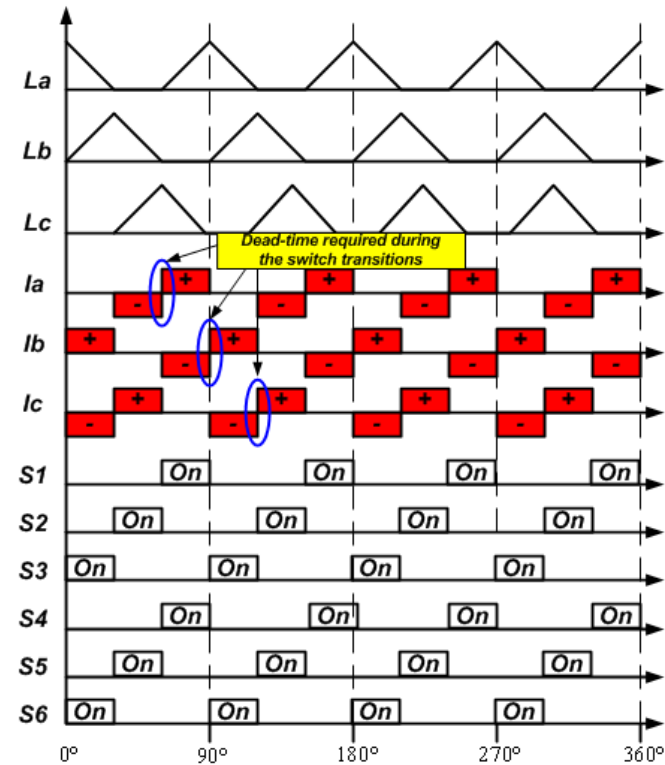


Fig. 5: Switching sequence for AFBC

As seen in the figure 5 the pulses for the switches of the full bridge converter are similar to half bridge but the signal is given to different switches. The common switches are given as S1S4, S2S5 and S3S6 to which simultaneous signals are fed. The direction of currents through the stator windings are changed with respect to signal fed to the switches. The gap between the pulses is same as that of half bridge converter with 30 degrees [9]. There is a dead time ΔD gap maintained between the pulses to avoid short circuit of the converter topology. The dead time ΔD is maintained as low as 2% of the complete time of full cycle.

$$\Delta D = 0.02 * T_s \dots\dots\dots(1)$$

Here Ts is the full cycle time, 0.02 represents 2%.

The asymmetrical half bridge switching sequence is further is updated with feedback loop controller as given in the figure 6 below.

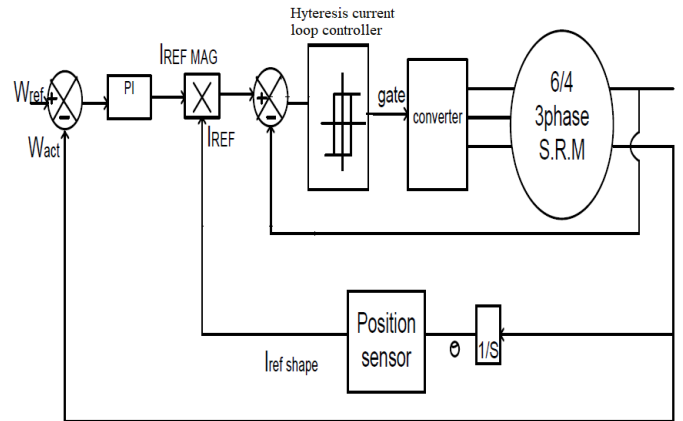


Fig. 6: Closed loop speed control of SRM with AHBC

In the above control structure, a speed feedback is taken from SRM represented as Wact (speed actual) compared to reference speed Wref generating speed error. The speed error is fed to PI controller with specific Kp (proportional gain) and Ki (Integral gain) values which generates reference current magnitude Irefmag [10]. The magnitude of the reference current generated from PI controller is multiplied with current measured with respect to position of the rotor. The rotor position sensor current estimator is shown below in figure 7.

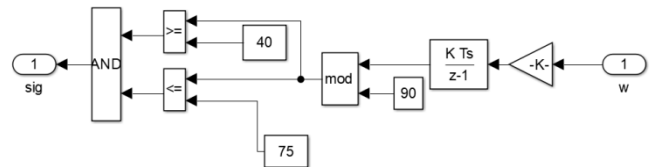


Fig. 7: Position sensor internal structure

The integration of rotor angle generates the position of the rotor. The rotor angle is given as

$$\delta = \frac{w+180}{\pi i} \dots\dots\dots(2)$$

Here, w is the rotor speed, the integral multiple 180/pi is conversion of radians to degrees.

A modulus function is applied to detect the position of the rotor. A signal is generated by comparison with two angle set points one greater than 30 degrees and one less than 90 degrees. A signal is generated only when the rotor position is between the limits (40 and 90 degrees). The Iref signal is multiplied with the current magnitude from the PI controller. The resultant current is compared to measured winding currents of SRM and the error is fed to hysteresis current loop controller [11]. The hysteresis controller generates pulses with respect to upper bound and lower bound limits given as per the user. The pulse generation by the hysteresis current loop controller is shown below.

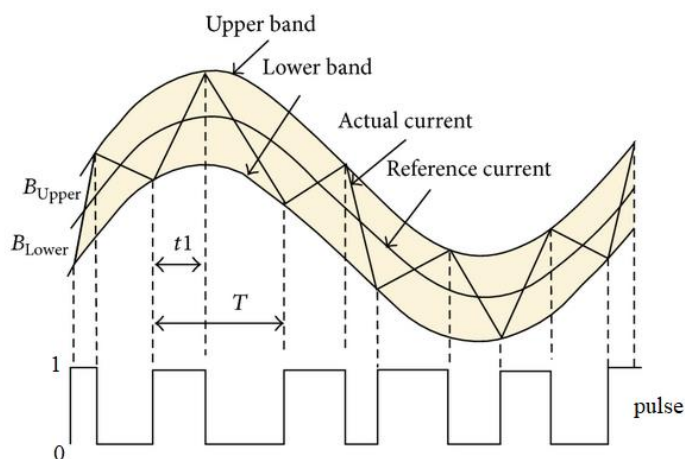


**Fig. 8:** Hysteresis current loop controller

As seen in the above figure 8 whenever the actual current is greater than reference current and the comparison value crosses the upper bound limit a signal '0' LOW is generated. And when the actual current is less than reference current and the comparison value cross the lower bound limit a signal '1' HIGH is generated [11]. The resultant pulse is fed to simultaneous switches in each leg. Each current signal comparison controls each phase switches.

**4. Simulation Results And Discussion**

With the above circuit topologies and SRM module modeling of the circuits are done in MATLAB Simulink environment. The open loop pulses for the AHBC are shown below.

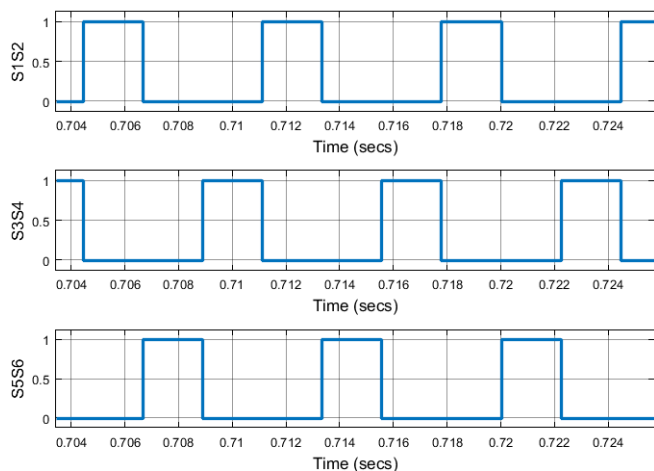


**Fig. 9:** Open loop pulses for AHBC

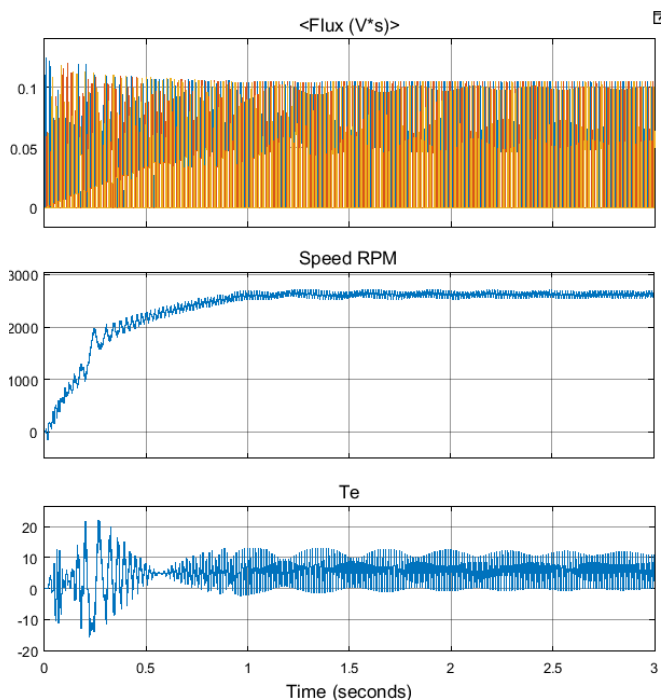


**Fig. 10:** SRM characteristics with open loop control of AHBC

The above are the SRM characteristics when the motor is run on AHBC. The complete full cycle time is set to 20msec where each set of switches operate for 6.66msec. The same full cycle time pulses are fed to AFBC as shown below and the characteristics of SRM are shown in figure 12.

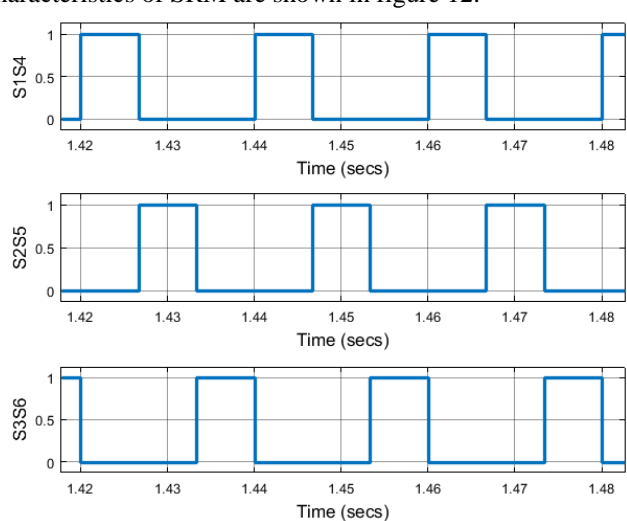


**Fig. 11:** Open loop pulses for AFBC

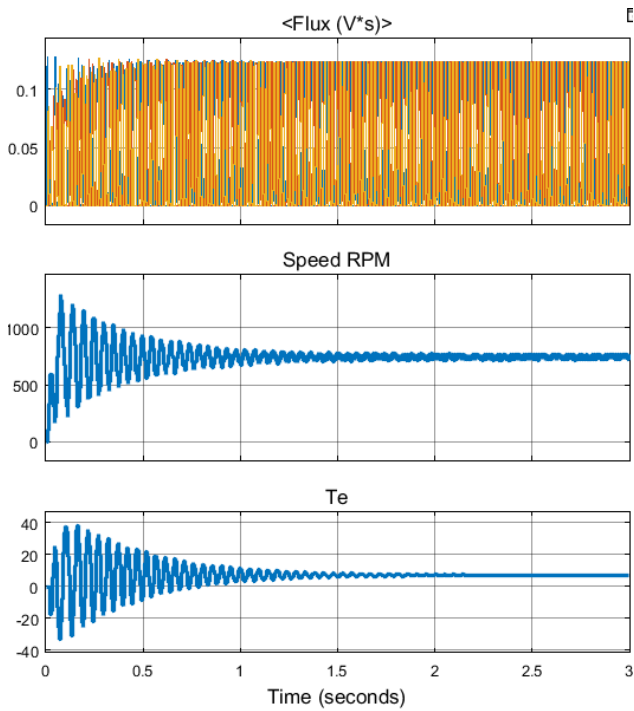


Fig. 12: SRM characteristics with open loop control of AFBC

The AHBC with SRM is updated with feedback closed loop control and modeled in Simulink as below.

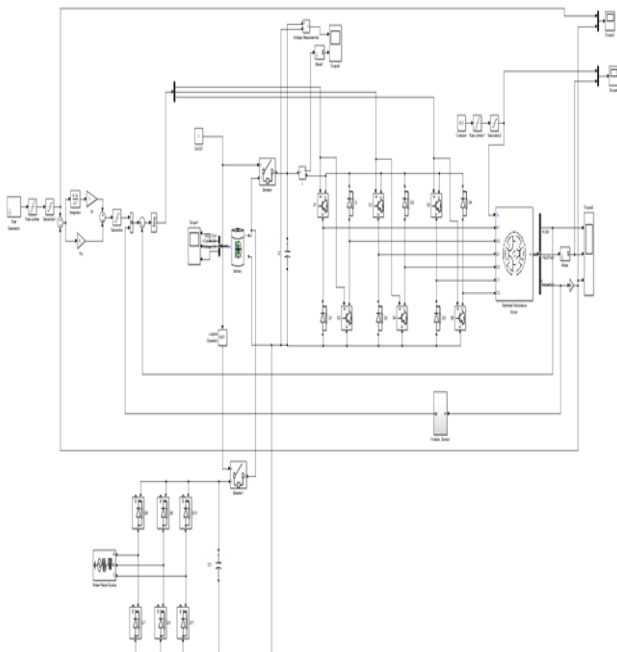


Fig. 13: Speed controller of SRM using AHBC

The converter is included with an EV battery charging circuit which had three phase source connected to diode bridge rectifier which charges the EV battery. The charge and discharge control is achieved by two breaker operating complementarily as per the user requirement. During discharge mode the speed reference and actual speed of the SRM is shown below. As seen the reference speed is slowly raised

from 0 to 1000rpm in time from 0-0.1sec and speed is slowly changed to -1000rpm at 0.5sec.

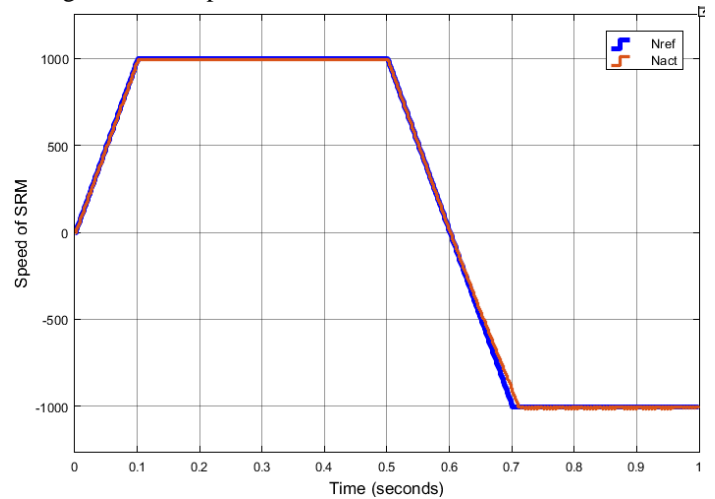


Fig. 14: Speed comparison with reference and actual signal with  $K_p = 1$  and  $K_i = 5$ .

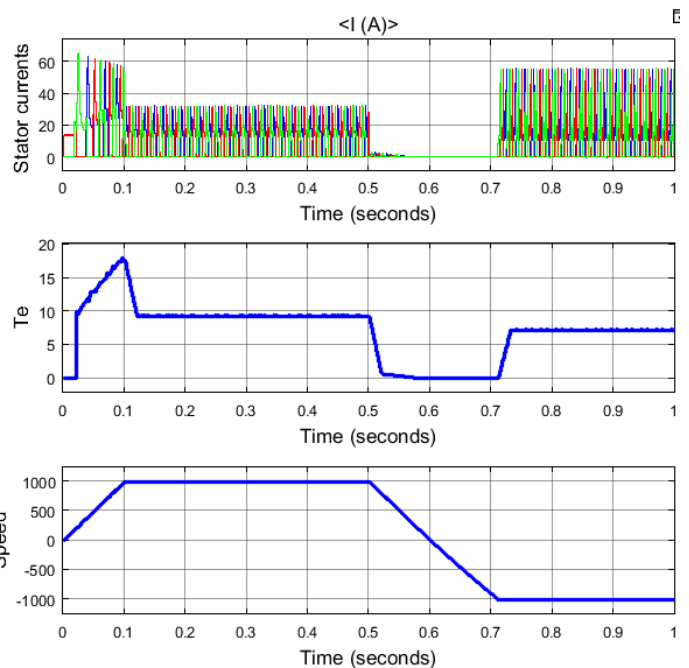


Fig. 15: SRM characteristics with speed control ( $K_p=1$ ,  $K_i = 5$ )

The above are the SRM characteristics with speed control with change in speed reference from 1000rpm to -1000rpm. The speed controller  $K_p$  and  $K_i$  values are adjusted and the difference in the characteristics of the SRM are observed. The above figures 14 and 15 are the characteristics of SRM with  $K_p$  and  $K_i$  values set at 1 and 5 respectively. The values are changed to 0.05 and 0.1 and the characteristics of SRM are shown below.

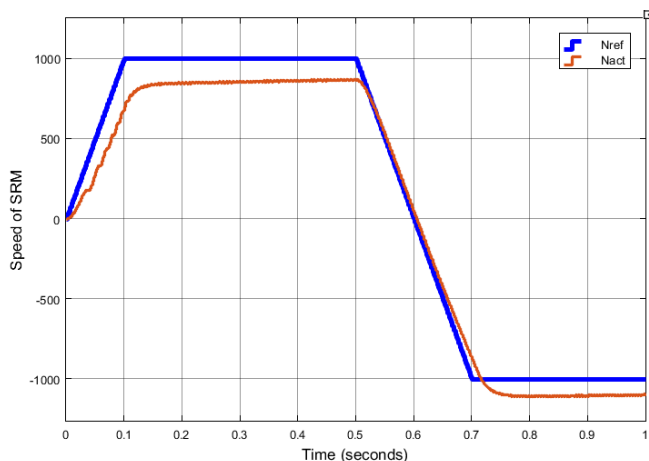


Fig. 16: Speed comparison with reference and actual signal with  $K_p = 0.05$  and  $K_i = 0.1$

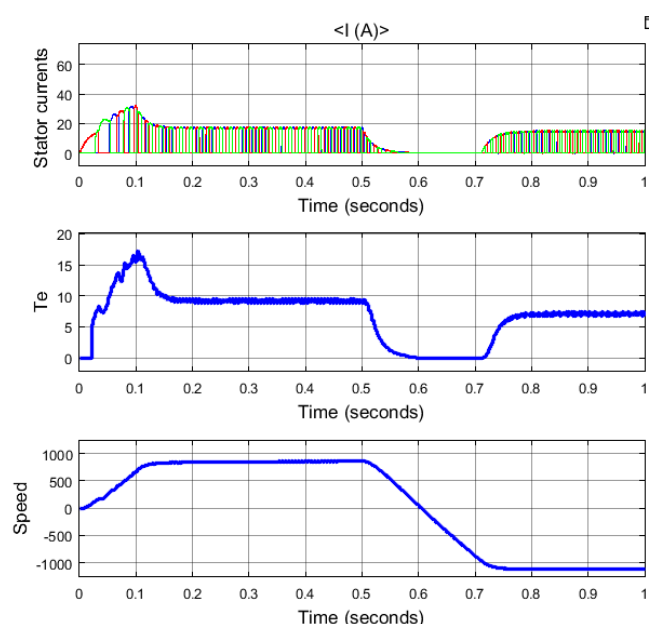


Fig. 17: SRM characteristics with speed control ( $K_p=0.05$ ,  $K_i = 0.1$ )

The  $K_p$  and  $K_i$  values are further updated to  $K_p = 50$  and  $K_i = 500$  and the characteristics are recorded as below.

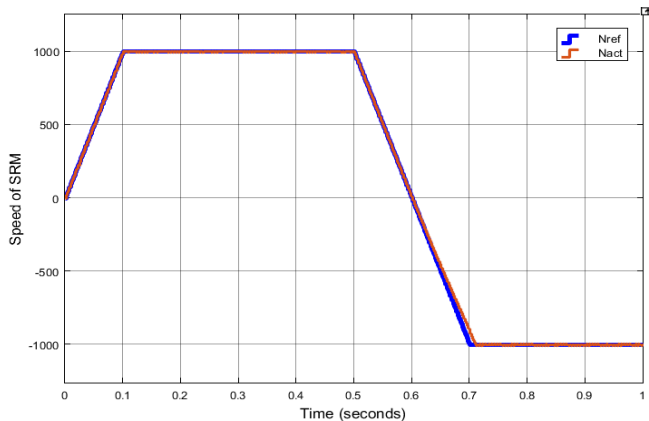


Fig. 18: Speed comparison with reference and actual signal with  $K_p = 50$  and  $K_i = 500$

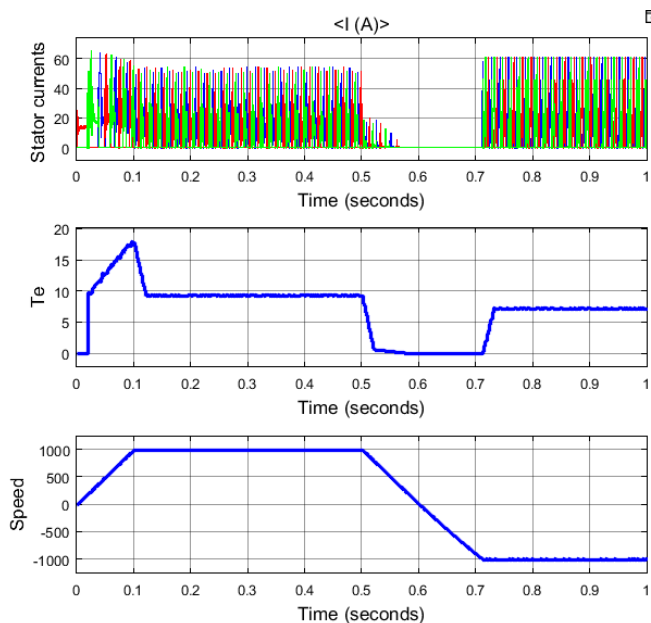


Fig. 19: SRM characteristics with speed control ( $K_p=50$ ,  $K_i = 500$ )

With the above results comparison the  $K_p$  and  $K_i$  values for the speed control needs to be considered above 1 and 5 respectively. The value below these does not generate accurate speed result for the SRM.

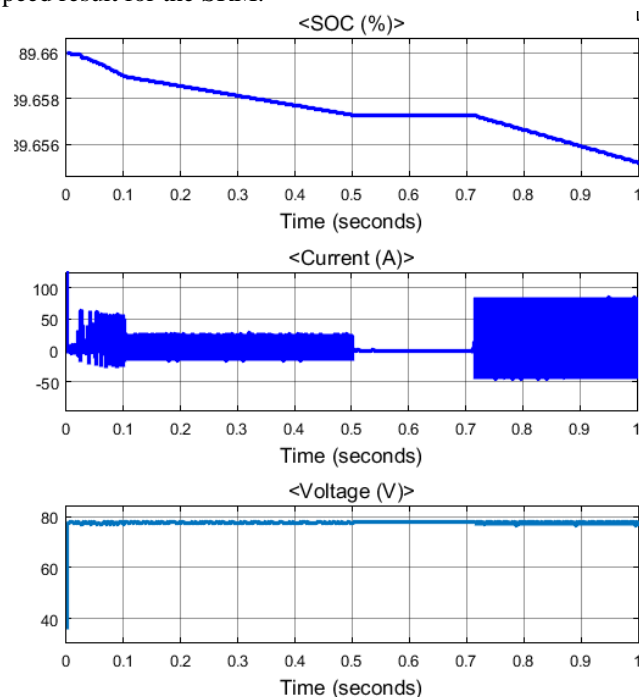


Fig. 16: EV battery discharge mode characteristics

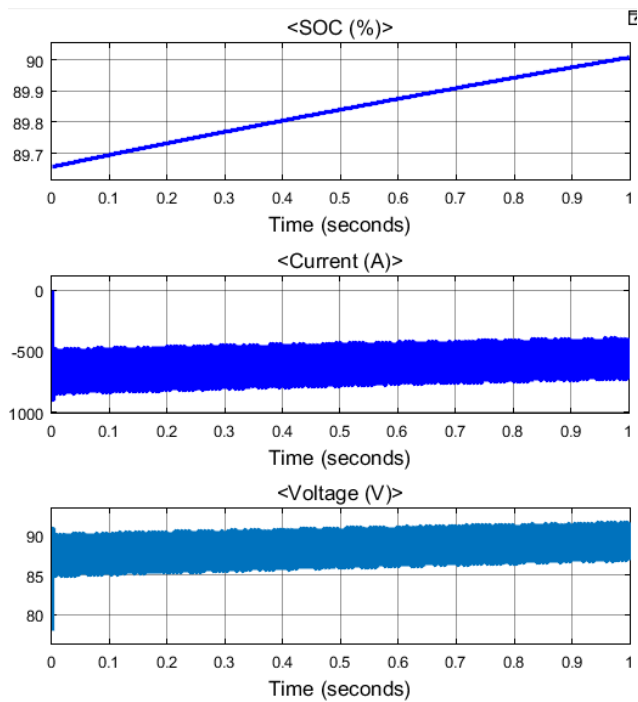


Fig. 17: EV battery charge mode characteristics

Different operating modes (discharge and charge modes) with the breaker ON and OFF conditions are simulated and EV battery characteristics are shown in figure 16 and 17.

## 5. Conclusion

With the above results it is determined that the speed and electro-magnetic torque of the SRM is more stable for AFBC. However, there is a risk of short circuit when two switches in the same leg operate simultaneously. The pulses need dead time gap between each other for the converter to operate with fault in the system. The AHBC is less risky and easy to control and hence a feedback closed loop control is developed for the AHBC. The SRM characteristics with different speed references are shown where the speed varies from 1000rpm to -1000rpm.

## APPENDIX

6/4 SRM parameters

$V_{in} = 72V$ ,  $I_{rated} = 65amps$ ,  $Inertia = 0.0082kg\cdot m^2$ ,  $R_s = 72/65$  ohms.

Battery parameters

Type - Lithium ion battery,  $V_{bat}$  nominal = 72V, Rated capacity = 50Ahr.

## References

- [1] R. Krishnan, *Switched Reluctance Motor Drives*, CRC Press, 2001.
- [2] A. C. Clothier, B. C. Mecrow, "The use of three phase bridge inverters with switched reluctance drives," *IEEE Electrical Machines and Drives Conference*, PP 351-355, 1997.

- [3] J. W. Ahn, S. G. Oh, J. W. Moon, Y. M. Hwang, "A three-phase switched reluctance motor with two-phase excitation," *IEEE Trans. Ind. Applicat.*, Vol.35, PP 1067 – 1075, 1999
- [4] Y. C. Kim, Y. H. Yoon, B. K. Lee, J. Hur, C. Y. Won, "A new cost effective SRM drive using commercial 6-switch IGBT modules," *IEEE Power Electronics Specialists Conference*, PP 1-7, 2006.
- [5] S.A. Nasar, "DC Switched Reluctance Motor", *Proceedings of the Institution of Electrical Engineers*, vol. 166, no.6, June, 1996, pp. 1048-1049.
- [6] J.V. Byrne, et al., "A High Performance Variable Reluctance Drive: A New Brushless Servo", *Motor Control Proceedings*, Oct. 1985, pp. 147-160.
- [7] P.French and A.H. Williams, "A New Electric Propulsion Motor", *Proceedings of AIAA Third Propulsion Joint Specialist Conference*, Washington, D.C., July, 1967.
- [8] L.E. Unnewehr and H.W. Koch, "An Axial Air-Gap Reluctance motor for Variable Speed Application", *IEEE Transactions on Power Apparatus and Systems*, vol.PAS-93, no.1, January, 1974, pp. 367-376.
- [9] P.J. Lawrenson, "Switched Reluctance Motor Drives", *Electronics and Power*, 1983, pp. 144-147.
- [10] R. Krishnan, "Switched Reluctance Motor Drives: Modeling, Simulation, Analysis, Design, and Applications", CRC Press, 2001.
- [11] T. J. E. Miller. "Electronic control of switched reluctance motors". *Newnes Power Engineering Series Oxford, UK*, 2001